

1 RNA-Seq Time Series of *Vitis vinifera* Bud 2 Development Reveals Correlation of Expression 3 Patterns with the Local Temperature Profile

4 Boas Pucker^{1,3}, Anna Schwandner², Sarah Becker¹, Ludger Hausmann², Prisca Viehöver¹,
5 Reinhard Töpfer², Bernd Weisshaar¹, and Daniela Holtgräwe^{1,*}

6
7 ¹ Genetics and Genomics of Plants, Faculty of Biology and Center for Biotechnology (CeBiTec), Bielefeld
8 University, Bielefeld, Germany; bpucker@cebitec.uni-bielefeld.de (B.P.), sabecker@techfak.uni-bielefeld.de
9 (S.B.), viehoeve@cebitec.uni-bielefeld.de (P.V.), bernd.weisshaar@uni-bielefeld.de (B.W.),
10 dholtgra@cebitec.uni-bielefeld.de (D.H.)

11 ² Julius Kühn-Institute (JKI), Institute for Grapevine Breeding Geilweilerhof, Siebeldingen, Germany;
12 anna.schwandner@julius-kuehn.de (A.S.), ludger.hausmann@julius-kuehn.de (L.H.),
13 reinhard.toepfer@julius-kuehn.de (R.T.)

14 ³ Evolution and Diversity, Department of Plant Sciences, University of Cambridge, Cambridge, United
15 Kingdom; bpucker@cebitec.uni-bielefeld.de (B.P.)

16 * Correspondence: dholtgra@cebitec.uni-bielefeld.de (D.H.)
17 ORCIDs: BP 0000-0002-3321-7471; AS 0000-0001-8755-1435; LH 0000-0002-4046-9626; RT 0000-0003-1569-
18 2495; BW 0000-0002-7635-3473, DH 0000-0002-1062-4576.

19 Received: date; Accepted: date; Published: date

20 **Abstract:** Plants display sophisticated mechanisms to tolerate challenging environmental conditions
21 and need to manage their ontogenesis in parallel. Here, we set out to generate an RNA-Seq time
22 series dataset throughout grapevine (*Vitis vinifera*) early bud development. The expression of the
23 developmental regulator *VviAP1* served as an indicator for progress of development. We
24 investigated the impact of changing temperatures on gene expression levels during the time series
25 and detected a correlation between increased temperatures and a high expression level of genes
26 encoding heat-shock proteins. The data set also allowed the exemplary investigation of expression
27 patterns of genes from three transcription factor (TF) gene families, namely MADS-box, WRKY, and
28 R2R3-MYB genes. Inspection of the expression profiles from all three TF gene families indicated that
29 a switch in the developmental program takes place in July which coincides with increased
30 expression of the bud dormancy marker gene *VviDRM1*.

31
32 **Keywords:** grapevine; ontogenesis; gene expression; AP1; DRM1; MYB; WRKY; MADS-box; HSP;
33 heat-shock genes; qRT-PCR reference genes
34

35 1. Introduction

36 Plants are sessile organisms which cannot escape from herbivores or changes in environmental
37 conditions. As a consequence, various stress response mechanisms [1,2] and complex specialized
38 metabolite pathways evolved to counteract adverse situations and conditions [3,4]. These response
39 mechanisms also need to protect plant embryogenesis, as well as vegetative developmental processes
40 like outgrowth of side shoots from resting or latent buds. All these developmental processes,
41 including the establishment of compound buds, have to proceed undisturbed despite potentially
42 challenging and/or unfavorable environmental conditions.

43 Similar to other woody perennial plants like e.g. apple or poplar, *V. vinifera* (grapevine) bud
44 development spans over two years between bud initiation and growth of new side shoots. Newly
45 formed buds enter in a dormancy phase in the winter time between the two growing seasons before

46 buds sprout in the second season [5,6]. In spring of the first season (April/May on the northern
47 hemisphere), new axillary buds are formed on young grapevine shoots. These new buds initially
48 contain meristems that develop into embryonic shoots with their shoot apical meristems (SAM) and
49 containing primordia for leaves, tendrils and inflorescences. This implies that different types of
50 meristems, including lateral and inflorescence meristems, co-exist in the buds. Floral transition takes
51 place at about June, five to seven weeks after burst of "old" buds (i. e. the buds that are one year ahead
52 in development). Inflorescence primordia differentiate from uncommitted primordia formed within
53 the new buds. Due to further differentiation of inflorescence meristems into inflorescence branch
54 meristems (about July), the compound buds finally contain the embryonic version of next year's
55 shoots, each with tissues for first leaves, inflorescences and tendrils [6,7]. The buds enter
56 endodormancy which passes over into ecodormancy depending on the environmental conditions of
57 fall and winter [8-10]. In early spring of the second season, ecodormancy is released and inflorescence
58 branch meristems produce single flower meristems in swelling buds (April) and flower organ
59 development begins [6]. It is important to note that the precise timing of floral transition and
60 development strongly depend on environmental conditions and genotype.

61 Heat-shock proteins (HSPs) are a group of proteins, which were initially detected due to their
62 accumulation in response to quickly increased temperature. They realize a molecular mechanism to
63 endure higher temperatures. First reports of HSPs in plants reach back to the 1980s when they were
64 described based on cell culture experiments with tobacco and soybean [11]. HSPs are assumed to
65 support several physiological functions under normal growth conditions. This includes folding,
66 unfolding, localization, accumulation and degradation of other proteins [12,13]. Additionally,
67 irreversible aggregation of other proteins is prevented and refolding is facilitated under heat stress
68 [14]. Several categories of HSPs based on sequence homology and typical molecular weight have been
69 defined [12], thus leading to multiple polyphyletic groups of HSPs.

70 WRKY transcription factors (TFs) are a family of TFs, which play an important role in the
71 regulation of responses to environmental stress conditions [15-17]. R2R3-MYB TFs are often
72 responsible for controlling the formation of specialized metabolites in response to environmental
73 triggers, but also regulate several plant-specific processes including root hair and trichome
74 differentiation [18-20]. MADS-box TFs are typically involved in the regulation of developmental
75 processes like determination of plant organ identity [21-23]. One especially important developmental
76 regulator is APETALA1 (AP1), also a MADS-box factor, which connects signals received from the
77 environment with initiation and/or progress of developmental processes [24,25]. *VviAP1* and
78 *VviAIL2*, a *V. vinifera* homolog of the MADS-box gene *AINTEGUMENTA-like* (*AtAIL1*, At1g72570),
79 have been postulated to be involved in the photoperiodic control of seasonal growth [26]. In addition,
80 marker genes for the dormant state of buds have been described. One such marker gene is *DRM1*, a
81 gene that has been found initially in *Pisum sativum* to encode a dormancy-associated protein [27].
82 Subsequently, *DRM1* homologs have been identified in many species in the context of bud dormancy,
83 including *V. vinifera* [10,28].

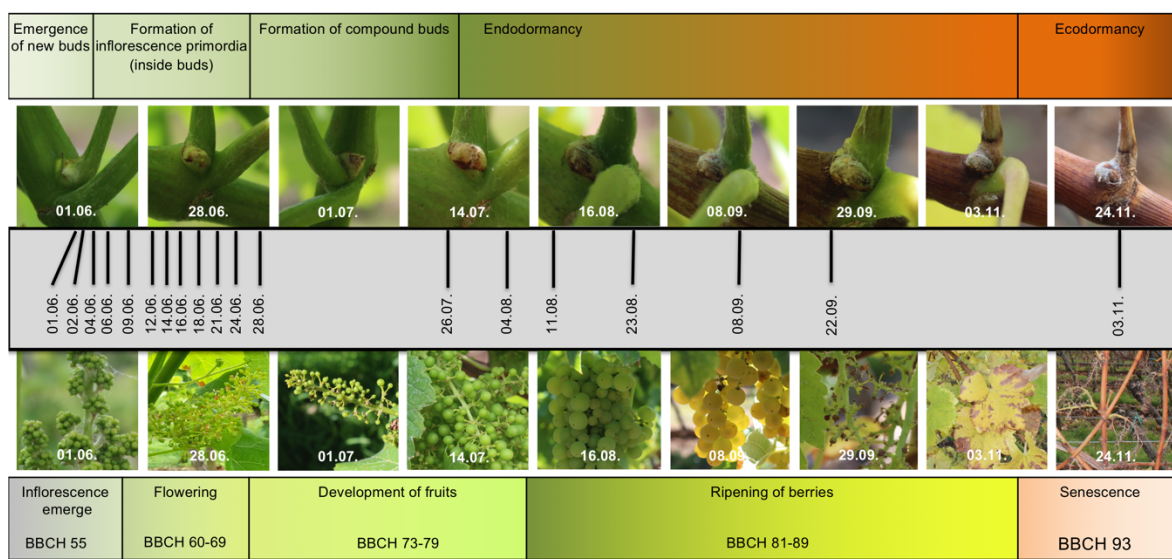
84 In the model plant *Arabidopsis thaliana*, phylotranscriptomic evidence for a molecular embryonic
85 hourglass was published [29-31]. We attempted to create an RNA-Seq dataset to examine early bud
86 development of *V. vinifera* for a similar general pattern. While an hourglass pattern was not detected
87 in the data (M. Quint, personal communication), we harnessed the time series of *V. vinifera* RNA-Seq
88 samples to investigate changes in gene expression during early bud development throughout the first
89 season at a fine scale and observed a strong influence of high temperatures on the expression of HSP
90 genes of field grown plants. In addition, a switch in the expression patterns of various TF genes was
91 observed that happens in parallel to or shortly after the switch from uncommitted primordia to
92 inflorescence primordia. This switch in expression pattern coincides with onset of expression of the
93 dormancy marker gene *VviDRM1*.

94

95 2. Results

96 2.1. RNA-Seq Time Series of Early Bud Development and Transcript Accumulation Patterns of Selected
97 Marker Genes

98 Young buds of *V. vinifera* ‘Calardis Musqué’ were harvested in a vineyard in the south of
99 Germany over a period of 156 days of the first season of development, covering the time from June
100 1st to November 3rd of 2016 (Figure 1) (File S1). Per time point, buds derived from three vines were
101 harvested and subjected to RNA-Seq analyses in triplicates per time point. Values for gene
102 expression, inferred from values for transcript accumulation, were calculated for all transcribed
103 genes. (File S2, File S3, File S4; see methods for details). Time points with only two successful
104 biological replicates were included in the submission to the European Nucleotide Archive (ENA)
105 database (File S1), but excluded from the investigations presented here.
106

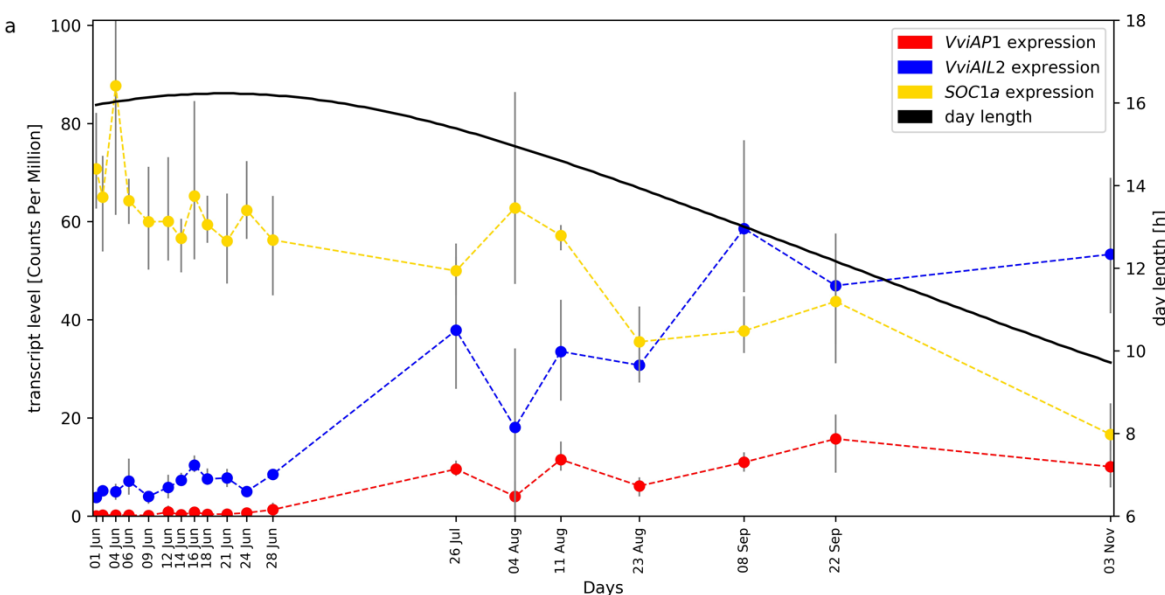


107

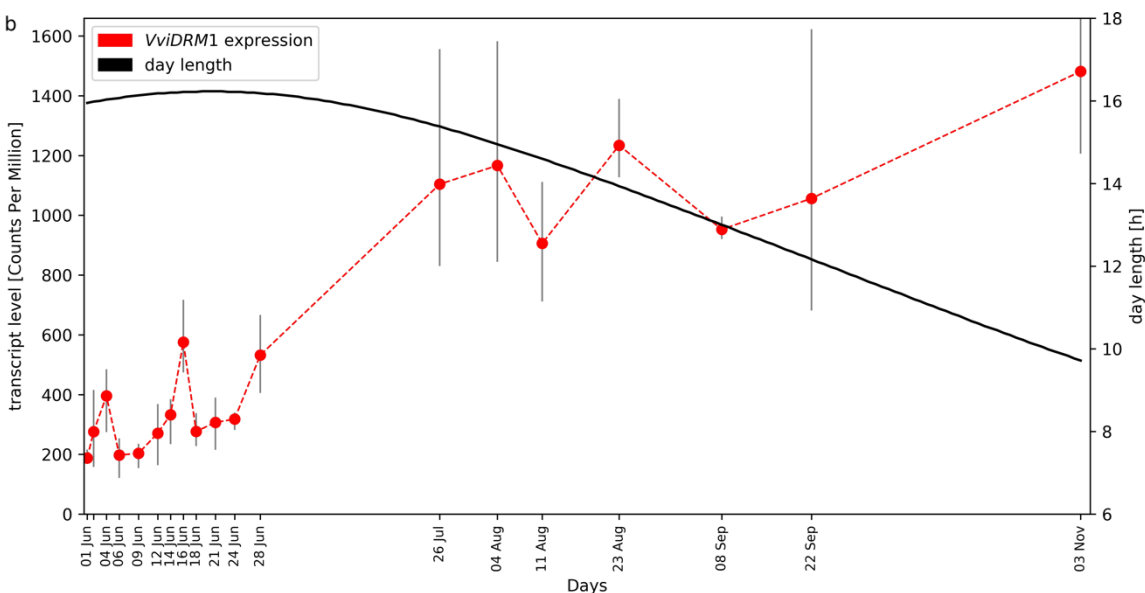
108 **Figure 1.** Documentation of the grapevine material used for sampling. The upper row of pictures displays the
109 bud stages during the first year of development, which were the target of this study. The lower row of pictures
110 displays the growth status of the vines from which the young buds were taken. In the center (grey bar), the
111 sampling time line is depicted.

112 The expression pattern of the MADS-Box genes *VviAP1* (CRIBI2.1 ID VIT_201s0011g00100),
113 *VviAIL2* (VIT_209s0002g01370), and *VviSOC1a* (VIT_215s0048g01250) are displayed in Figure 2a.
114 *VviAP1* transcript levels were zero or very low until end of June and rise until September. Due to the
115 time distance between the sampling points we interpret the data as essentially one peak in September.
116 *VviAP1* and *VviAIL2* display quite similar expression patterns. The increase of *VviAP1* transcript
117 levels at the end of June correlates with the time when floral transition, the differentiation of
118 uncommitted primordia into inflorescence primordia, took place. There is no direct correlation
119 between the transcript levels of *VviAP1* and *VviAIL2* with the day length, but the rise of transcript
120 levels coincides with the beginning of reduction of day length after midsummer. We also checked the
121 expression of the dormancy marker gene *VviDRM1* (VIT_210s0003g00090) and found high transcript
122 levels of this gene in the buds with a clear increase starting in July (Figure 2b).

123



124



125

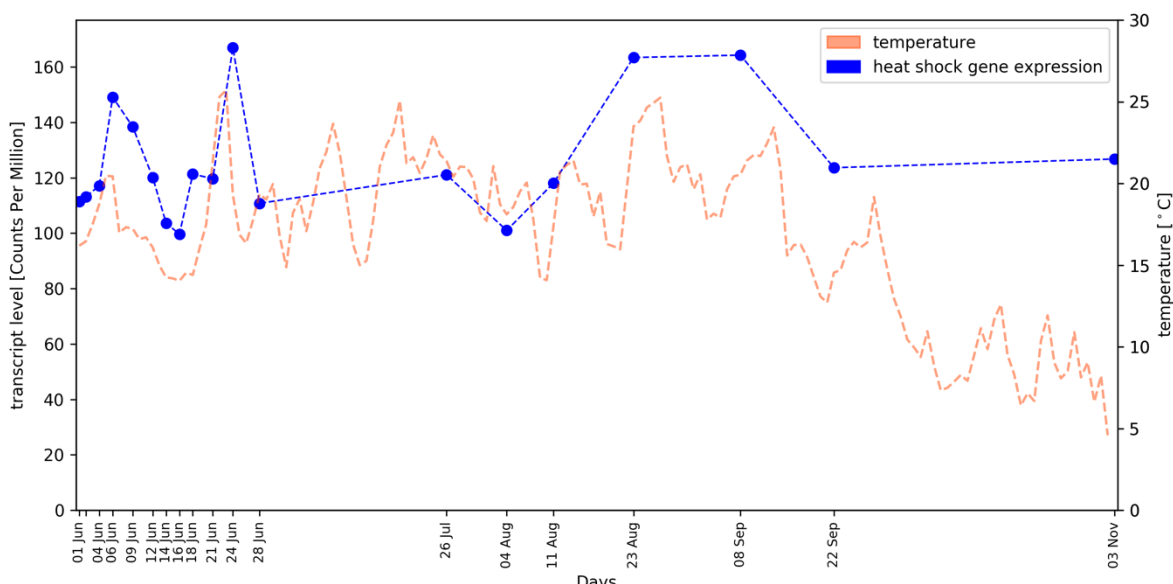
126 **Figure 2:** Gene expression time course of *VviAP1*, *VviAIL2*, and *SOC1a* (panel a) as well as *VviDRM1* (panel b) in developing grapevine buds. The plots were separated due to the large difference in
127 transcript levels (detected as standardized read counts), see y-axis on the left. Day length during the
128 sampling interval is plotted in both panels.
129

130

131 2.2. Average Gene Expression Values of HSP Genes Reflect the Local Temperature Profile

132 We made use of the weather data recorded at the vineyard from which the samples for RNA-
133 Seq were derived. Since the recorded temperature profile during 2016 displayed significant
134 oscillation, we tested the hypothesis that a heat-shock response may take place in the buds. A total of
135 131 putative HSP genes were identified based on the annotation (File S5), but only 80 of these show
136 substantial transcript abundance (CPM value of more than 10). The gene expression pattern of this
137 set of 80 HSP genes shows a good correlation ($r \approx 0.45$) with the temperature profile. Obviously, the
138 correlation is much better during the period with dense sampling. We observed clear HSP gene
139 transcript level peaks at time points with high temperatures (Figure 3). This is especially noticeable

140 at June 24th when the highest average temperature was recorded. A correlation of the day
141 length/photoperiod with the expression pattern of these genes was not observed.
142



143
144 **Figure 3:** Correlation of HSP gene expression (blue dots / blue dotted line) in developing grapevine
145 buds and environmental air temperature (red dashed line); the course of daily average
146 temperature values is shown.

147 2.3. Investigation of Transcription Factor Gene Families: WKRY, MADS-box, and R2R3-MYBs

148 We harnessed the presented RNA-Seq time series for the analyses of expression patterns of three
149 TF gene families. Heatmaps display transcript levels of genes encoding MADS-box (File S6), R2R3-
150 MYB (File S7), and WRKY (File S8) TFs. Only genes that display detectable transcript accumulation
151 values were considered (see Methods for the threshold). As can be seen from all three heatmaps, the
152 gene activity patterns of quite some of the transcription factor genes change quite dramatically with
153 the onset of *VviAP1* transcript accumulation between June 28th and July 26th.

154 While *VviSVP1* (VIT_200s0313g00070), an ortholog of the *A. thaliana* MADS-box gene *SHORT*
155 *VEGETATIVE PHASE/AGL22* (At2g22540), shows transcript levels with almost constant values, the
156 gene *VviFLC2* (VIT_214s0068g01800) displays a time course quite similar to those of *VviAP1* and
157 *VviAIL2*. *VviFLC2* is, like its paralog *VviFLC1* (VIT_201s0010g03890), closely related to the *A. thaliana*
158 MADS box gene *FLOWERING LOCUS C/AGL25* (At5g10140) which encodes a central repressor of the
159 floral transition. In contrast, *VviTM8a* (VIT_217s0000g01230), which was named according to a gene
160 initially detected in *Solanum lycopersicum* (*TOMATO MADS 8*) that became "founder" of a specific
161 sub-clade of evolutionary related MADS-box genes, shows a transcript accumulation peak at the end
162 of June. Finally, *VviSOC1a* (VIT_215s0048g01250), a homolog of the *A. thaliana* MADS box gene
163 *SUPPRESSOR OF OVEREXPRESSION OF CO 1/AGL20* (At2g45660) displays transcript
164 accumulation values that decline after middle of August (Figure 2a).

165 With regard to the R2R3-MYB genes, *VviMYBC2-L1* (VIT_201s0011g04760), *VviMYB4A*
166 (VIT_203s0038g02310), and *VviMYBPAR* (VIT_211s0016g01300) are prominent examples of genes
167 that support the gene expression pattern switch during July. In addition to the July switch, several
168 R2R3-MYB genes display high transcript accumulation values specifically in November. Clear
169 examples are *VviMYB15* (VIT_205s0049g01020), *VviMYB14* (VIT_205s0049g01020), and *VviMYB30A*
170 (VIT_217s0000g06190). Based on its high transcript levels, *VviMYBPA1* (VIT_215s0046g00170), a
171 homolog of the *A. thaliana* R2R3-MYB genes *TRANSPARENT TESTA 2/AtMYB123* (At5g35550) and
172 *AtMYB5* (At3g13540), appears as an important regulator. It is worth noting that another homolog of
173 *AtMYB123* and *AtMYB5*, namely *VviMYBPAR*, also shows high transcript levels from end of August
174 to September. Another R2R3-MYB gene that stands out due to high transcript levels is *VviMYB174*.

175 (VIT_218s0001g09850), a homolog of *AtMYB73* (At4g37260) and *AtMYB77* (At3g50060). As expected
176 for organs/tissue not accumulating anthocyanins, *VviMYBA1* (VIT_202s0033g00410), an ortholog of
177 the *A. thaliana* R2R3-MYB gene *PRODUCTION OF ANTHOCYANIN PIGMENT 1/AtMYB75*
178 (At1g56650), is not significantly expressed in young buds.

179 Several genes encoding TFs of the WRKY type show a substantial increase of transcript levels at
180 the gene expression pattern switch during July (e.g. *VviWRKY20* (VIT_207s0005g02570) or
181 *VviWRKY31* (VIT_210s0003g02810)). Examples for the opposite change, i.e. reduction of transcript
182 levels during July, are *VvWRKY23* (VIT_207s0031g01840) and *VviWRKY41* (VIT_213s0067g03140).
183 High transcript levels that are strongly reduced towards winter were detected for *VviWRKY25*
184 (VIT_208s0058g01390) that is, together with *VviWRKY41*, homologous to *AtWRKY54* (At2g40750),
185 *AtWRKY70* (At3g56400) and *AtWRKY46* (At2g46400). Like some of the R2R3-MYB genes, also several
186 *VviWRKY* genes display high transcript accumulation values specifically in November and/or an
187 increase towards winter. These include *VviWRKY16* (VIT_206s0004g07500), *VviWRKY45*
188 (VIT_214s0108g01280) and *VviWRKY33* (VIT_211s0037g00150) that are all homologous to the *A.*
189 *thaliana* WRKY genes of group I-C including *AtWRKY33* (At2g38470), *AtWRKY58* (At3g01080), and
190 *AtWRKY32* (At4g30935).

191 2.4. Identification of qRT-PCR Reference Genes

192 The quite long RNA-seq time series from tissue of compound buds, covering changing day
193 length and oscillating weather conditions in the field, allowed the identification of candidate
194 reference genes for quantitative Real-Time PCR (qRT-PCR) experiments. The 20 best candidates for
195 reference genes in qRT-PCR experiments were predicted based on an overall high expression and a
196 low variation in steady-state transcript abundance (File S9). A manual inspection of the functional
197 annotation of these genes supported the quality of this data set since it covers well-known qRT-PCR
198 reference genes like 'polyubiquitin', 'glyceraldehyde-3-phosphate dehydrogenase', 'elongation factor
199 Tu', and 'actin' as top candidates. The most promising candidate is *VviUBQ10* (VIT_219s0177g00040)
200 which is homologous to the five *A. thaliana* genes encoding polyubiquitin (At4g05320 and others).
201 The second best candidate is VIT_219s0015g01090, a homolog of *A. thaliana* HEAT SHOCK PROTEIN
202 81.4 (At5g56000).

203 3. Discussion

204 This time series of 18 RNA-Seq data points throughout the first year of development of *V. vinifera*
205 compound buds allows the investigation of developmental processes at relatively high resolution. A
206 similar time series analyses has been performed previously with Affymetrix arrays to determine gene
207 expression patterns for the cultivar Tempranillo [9]. While the data from Tempranillo that was grown
208 near Madrid cover the time from May (first year) to April (second year) with 8 time points, the focus
209 of the time series presented here was the early bud development in June until November of the first
210 year. Nevertheless, the previously reported expression pattern changes in July and also towards
211 winter (November time point) [9] were essentially matched by our data set.

212 Our chronologically dense collection of samples allows the detection of small developmental
213 differences between time points, but it is affected by a high variation through individual differences
214 between plants, sampled buds, and varying environmental conditions like temperature and other
215 weather conditions. Harvesting the buds in the field is technically challenging since the buds are
216 small and need to be cut out of the axil between shoot and leave or from hard wood. The sampling
217 has to be performed quickly and there was no time to remove adhering tissue from shoots before
218 freezing the samples in liquid nitrogen. The results presented were derived from data of the year
219 2016 and from time points for which three independent biological replicates were available.
220 However, there are more data of time points for which individual replicates were lost mainly during
221 the RNA extraction procedures due to the problematic technical properties of the respective samples
222 (File S1). While these time points should not be used for statistical analyses, they still provide
223 additional support for patterns observed or may increase the power of co-expression analyses in the
224 future.

225 Predicted reference genes for qRT-PCR experiments of bud samples contain commonly used
226 reference genes like GAPDH, actin, polyubiquitin, and elongation factor Tu. Additionally, novel
227 candidate genes were identified which displayed a constant expression level. This aligns well with a
228 previous study, which reported that novel reference genes identified by genome-wide *in silico*
229 analysis outperformed typical reference genes in common wheat [32].

230 We selected three well-known and in the model plant *A. thaliana* well-characterised TF gene
231 families for more detailed analyses of gene expression patterns. MADS-box genes were selected
232 because of their relation to development, and also because quite some of these genes were analysed
233 in the Tempranillo study of Diaz-Riquelme et al. [9]. R2R3-MYB genes and WRKY genes were
234 selected because of their link to stress responses as well as control of accumulation of specialized
235 metabolites.

236 The gene *VviSOC1a*, a potential integrator of multiple flowering signals that cumulate in the
237 establishment of inflorescence meristems [33], is expressed in June and expression declines after
238 middle of August, when *VviAP1* and also *VviLFY/VviFL* (VIT_217s0000g00150, see File S3; ortholog
239 of *AtLEAFY* [34], At5g61850) show increasing expression levels. This increased expression of
240 potential inflorescence meristem identity genes (*AP1*, *LEAFY*) coincides with proliferation of
241 inflorescence primordia, giving rise to inflorescence branch primordia in the developing compound
242 buds [5,6,35]. Based on the also increasing expression of the dormancy marker gene *VviDRM1*, it can
243 be postulated that other parts of the compound bud are already in July on their way to
244 endodormancy. Also the gene *VviTM8a*, a homolog of *TOMATO MADS 8* that plays a role in tomato
245 flower development [36], displays an interesting expression pattern that hints at inflorescence
246 developmental processes taking place during June and beginning of July.

247 With respect to the expression of the two R2R3-MYB factors known to control proanthocyanidin
248 (PA) biosynthesis that displayed conspicuous expression patterns, namely *VviMYBPA1* and
249 *VviMYBPAR* [37,38], three prominent potential target genes *VviLAR1* (VIT_201s0011g02960) *VviANS*
250 (or *VviLDOX*, VIT_202s0025g04720) and *VviANR* (VIT_200s0361g00040) show expression patterns
251 expected for targets (File S3), also with a reduction of expression levels towards winter. The three
252 genes encode the enzymes leucoanthocyanidin reductase (LAR), anthocyanidin synthase (ANS, also
253 referred to as LDOX) and anthocyanidin reductase (ANR) which are required for biosynthesis of
254 catechin and epicatechin that are precursors of PAs [38]. This indicates that the compound buds
255 accumulate PAs during summer and fall in preparation for winter. Similarly, it is conceivable that
256 the activation of *VviMYB14* and *VviMYB15* results in the synthesis of stilbenes [39,40], which fits to
257 the activation of three of the *V. vinifera* stilbene synthase genes [41] that are clustered on chromosome
258 16. While *VviSTS35* (VIT_216s0100g01070) and *VviSTS41* (VIT_216s0100g01130) might be targets of
259 *VviMYB15* based on strong co-expression in November, *VviSTS36* (VIT_216s0100g01100) fits better
260 as a potential target of *VviMYB14*. The analysis of *VviSTS* genes [41] also covered three *VviCHS* genes
261 (*VviCHS3*: VIT_205s0136g00260, *VviCHS1*: VIT_214s0068g00920 and *VviCHS2*: VIT_214s0068g00930).
262 The three *VviCHS* genes are co-expressed with a pattern similar to that of *VviLAR1*, *VviANS* and
263 *VviANR* which fits the substrate requirement for catechin/epicatechin biosynthesis and to
264 *VviMYBPA1* and/or *VviMYBPAR* as potential regulators. The homologs of the highly expressed gene
265 *VviMYB174*, *AtMYB73* and *AtMYB77*, have been implicated in root-related auxin responses [42]. A
266 similar function of *VviMYB174* would fit to its high expression throughout compound but
267 development from June to November.

268 Of the *VviWRKY* genes that have been implicated in the control of *VviSTS*'s, namely *VviWRKY03*,
269 *VviWRKY24*, *VviWRKY43* and *VviWRKY53* [40], only *VviWRKY03* (VIT_201s0010g03930) displayed
270 expression with a pattern that fits to that of *VviMYB14* and *VviSTS36*, allowing to hypothesize that
271 *STS36* expression is under combinatorial control of *MYB14/WRKY03* in compound buds.
272 *VviWRKY25*, and to some extent *VviWRKY41* as well, that are both homologous to the *AtWRKY* genes
273 implicated in brassinosteroid-regulated plant growth [43], show expression patterns that fit to growth
274 actions until September that are then abandoned towards November and winter.

275 To the best of our knowledge, this is the first report of a correlation between HSP gene expression
276 patterns with the environmental temperature in a comprehensive time series of field (vineyard)

samples. However, repeated formation of HSPs was previously described in the seeds, seed pods, and flowers of *Medicago sativa* [44]. The occurrence of HSPs at standard (not stressed) growth conditions indicated a potential role in development [44]. The annotation “heat-shock” was initially introduced based on up-regulation of genes in heat stress experiments [11,45]. HSPs were also detected at substantial levels in field-grown *Gossypium hirsutum* under increased temperature and drought stress [46]. Reports from *Oryza sativa* support the stress signal integration function of HSPs [47]. Therefore, we also checked for other stress factors like documented pathogen attack, crop protection treatments, or drought stress, but temperature was the only factor with a substantial correlation. Considering the large number of physiological functions of HSPs, constantly expressed chaperons might also be annotated as HSPs. The observation of constant high expression for a gene annotated as “heat-shock protein” (VIT_219s0015g01090) among the potential reference genes for qRT-PCR supports this hypothesis. This assumption aligns well with previous findings that HSPs can have functions in the integration of stress signals [48]. Since our analysis of HSPs is based on the currently available functional annotation, it is likely that the gene expression correlation of bona fide HSP genes with the temperature profile might be even stronger than described here. Moreover, it is possible that additional factors like an underlying developmental pattern or UV-B exposure have an additional influence on the observed heat-shock gene expression profile.

294

295 4. Materials and Methods

296 4.1. Biological Material

297 Buds of consecutive time points within the first year of their developmental cycle were taken
298 from a vineyard of the cultivar ‘Calardis Musqué’ (‘Bacchus Weiss’ x ‘Seyval’), former breeding line
299 GF.GA-47-42 (VIVC variety number 4549; <http://www.vivc.de>). The plot consists of 1300 vines,
300 planted in 1995, pruned as a single cane Guyot system, and located at the Institute for Grapevine
301 Breeding Geilweilerhof in Siebeldingen (49°13'05.0"N 8°02'45.0"E), about 120 m north of a weather
302 station (<https://www.am.rlp.de/Internet/AM/NotesAM.nsf/amwebagr/>). Early in the afternoon on
303 each sampling date of the growing season, bud samples were taken in triplicates. From three different
304 vines four buds each were harvested in a batch and immediately frozen in liquid nitrogen. The buds
305 were taken from the fourth to eight node of the shoots emerging from the middle section of the cane
306 (Figure 4). Vines that appeared to be equal in their overall developmental stage were chosen. Those
307 that showed symptoms of nutrient deficiency or diseases were excluded as a sample source.

308



309 **Figure 4:** The same vine of ‘Calardis Musqué’ on 1st of July and 16th of December 2016. White circles mark the
310 fourth to eight node of the middle shoots from which the buds were harvested.

311 4.2. RNA Extraction, Library Preparation, and Sequencing

312 Total RNA was extracted, from four buds each, in triplicate per time point. Up to 100 mg of
313 liquid nitrogen ground tissue was applied to the SpectrumTM Plant Total RNA kit (Sigma-Aldrich,
314 Taufkirchen, Germany) according to the manufacturer's instructions for protocol B. After on-column
315 DNase treatment with the DNase I Digest Set (Sigma-Aldrich, Taufkirchen, Germany), the RNA was
316 quantified. 500 ng total RNA per sample were used to prepare sequencing libraries according to the
317 Illumina TruSeq RNA Sample Preparation v2 Guide. Purification of the polyA-containing mRNA
318 was performed using two rounds of oligo(dT) oligonucleotides attached to magnetic beads. During
319 the second elution of the polyA+ RNA, the RNA was fragmented and primed for cDNA synthesis.
320 After cDNA synthesis, the DNA fragments were end-repaired and A-tailing was performed. Multiple
321 indexing adapters, specific for each library and sample, were ligated to the ends of the cDNA
322 fragments and the adapter ligated fragments were enriched by 12 cycles of PCR. After qualification
323 and quantification, the resulting sequencing libraries were equimolarly pooled and sequenced
324 generating 100 nt single-end reads on eight lanes of an Illumina HiSeq1500 flowcell at the Sequencing
325 Core Facility of the Center for Biotechnology (CeBiTec) at Bielefeld University.

326 *4.3. Bioinformatic Analysis of RNA-Seq Data*

327 All RNA-Seq read data sets generated were submitted to the ENA (for accession numbers see
328 File S1). Python scripts developed for customized analyses are available at Github:
329 <https://github.com/bpucker/vivi-bud-dev>. RNA-Seq reads were mapped to the CRIBI2.1 reference
330 genome sequence of PN40024 [49] via STAR v.2.51b [50] with previously optimized parameters
331 including a minimal alignment length cutoff of 90% and a minimal similarity cutoff of 95% of the
332 read length [51]. FeatureCounts [52] was deployed for quantification of steady-state transcript levels
333 at the gene level based on these mappings and the CRIBI2.1 annotation [53]. Previously developed
334 Python scripts [51] were applied to merge the resulting count tables and to calculate counts per
335 million (CPMs) and reads per kb per million mapped reads (RPKMs). We attempted to include *VviFT*
336 (GSVIVT00012870001 in the Vv8x genome sequence) in the analyses of selected target genes, but the
337 corresponding sequence region is not included in the genome sequence version (file Vv12x_CRIBI.fa)
338 on which the CRIBI2.1 annotation is based. To include the three *VviCHS* genes [41], structural gene
339 annotation was optimised for VIT_214s0068g00920 and VIT_214s0068g00930.

340 Average day temperature values were retrieved from the weather station in the vineyard for the
341 time from June 1st to November 3rd of 2016.

342 HSP genes in CRIBI2.1 were identified based on the annotation text of homologs in *A. thaliana*
343 by filtering for the strings 'heat' and 'shock' occurring together in the functional annotation text of
344 the genes. Lowly expressed genes were excluded from downstream analyses by applying a minimal
345 CPM cutoff of 10 (per gene sum over all samples). The Python package matplotlib v2.1.0 [54] was
346 used for visualization of the data.

347 Members of the transcription factor families WRKY [16], MADS-box [23], and MYB [19,39] were
348 identified based on the published gene family analyses. The *V. vinifera* WRKY gene family has also
349 been characterised by Guo et al. (2014) [55] which, unfortunately, resulted in conflicting gene
350 designations. For consistency with Vannozzi et al. [40] we only used the *VviWRKY* gene designations
351 of Wang et al. (2014). To allow the expression analysis of all previously described MADS-box genes,
352 the CRIBI v2.1 annotation was extended with corresponding gene models using "VIT_230_" as prefix
353 for the additional locus IDs. The Python packages matplotlib v2.1.0 [54] and seaborn v0.8.1
354 (<https://github.com/mwaskom/seaborn>) were used for visualization of RPKM values of selected
355 genes in heatmaps.

356 Candidates for reference genes suitable for qRT-PCR experiments in the future were identified
357 based on our comprehensive set of RNA-Seq samples. First, genes with a substantial expression level
358 defined as sum of all samples greater or equal to 500 [CPM] were selected. Second, these candidate
359 set was filtered for a low variation defined as small standard deviation values across all samples
360 normalized by the median of all values.

362 **Supplementary Materials:** The following files are available online at www.mdpi.com/xxx/s1:
363 File S1: RNA-Seq sample overview including ENA accessions and number of reads per sample,
364 File S2: Raw counts of RNA-Seq reads mapped to CRIBI2.1,
365 File S3: CPMs of RNA-Seq reads mapped to CRIBI2.1,
366 File S4: RPKMs of RNA-Seq reads mapped to CRIBI2.1,
367 File S5: IDs of potential heatshock genes in CRIBI2.1,
368 File S6: Gene expression heatmap of genes encoding MADS-box TFs,
369 File S7: Gene expression heatmap of genes encoding R2R3-MYB TFs,
370 File S8: Gene expression heatmap of genes encoding WRKY TFs,
371 File S9: List of candidates for qRT-PCR reference genes.
372

373 **Author Contributions:** DH, LH, RT and BW conceived and designed research. BP, AS, SB, and PV conducted
374 the experiments. BP, LH, DH and BW interpreted the data. BP, DH, and BW wrote the manuscript. All authors
375 read and approved the final version of the manuscript.

376

377 **Funding:** We acknowledge the financial support of the German Research Foundation (DFG, <http://www.dfg.de>)
378 to BW (WE1576/16-2) and to RT (TO152/5-2) in the context of SPP-1530. In addition, this paper is also based on
379 work from COST Action CA 17111 INTEGRAPE, supported by COST (European Cooperation in Science and
380 Technology).

381 **Acknowledgments:** We are grateful to Willy Keller for excellent technical assistance. In addition, the authors
382 wish to thank all members of the group "Genetics and Genomics of Plants" and the Bioinformatics Resource
383 Facility of the CeBiTec for their excellent assistance and support. We also acknowledge the financial support of
384 the German Research Foundation and the Open Access Publication Fund of Bielefeld University for the article
385 processing charge.

386 **Conflicts of Interest:** The authors declare no conflict of interest.

387

388 **References**

- 389 1. Bokszczanin, K.L.; Solanaceae Pollen Thermotolerance Initial Training Network, C.; Fragkostefanakis, S.
390 Perspectives on deciphering mechanisms underlying plant heat stress response and thermotolerance.
391 Frontiers in Plant Science 2013, 4, 315, doi:10.3389/fpls.2013.00315.
- 392 2. Basu, S.; Ramegowda, V.; Kumar, A.; Pereira, A. Plant adaptation to drought stress. F1000Research 2016, 5,
393 1554, doi:10.12688/f1000research.7678.1.
- 394 3. Caretto, S.; Linsalata, V.; Colella, G.; Mita, G.; Lattanzio, V. Carbon Fluxes between Primary Metabolism
395 and Phenolic Pathway in Plant Tissues under Stress. International Journal of Molecular Sciences 2015, 16,
396 26378-26394, doi:10.3390/ijms161125967.
- 397 4. Yang, L.; Wen, K.S.; Ruan, X.; Zhao, Y.X.; Wei, F.; Wang, Q. Response of Plant Secondary Metabolites to
398 Environmental Factors. Molecules 2018, 23, doi:10.3390/molecules23040762.
- 399 5. Carmona, M.J.; Chaib, J.; Martínez-Zapater, J.M.; Thomas, M.R. A molecular genetic perspective of
400 reproductive development in grapevine. Journal of Experimental Botany 2008, 59, 2579-2596,
401 doi:10.1093/jxb/ern160.
- 402 6. Vasconcelos, C.M.; Greven, M.; Winefield, C.S.; Trought, M.C.T.; Raw, V. The Flowering Process of *Vitis*
403 *vinifera*: A Review. American Journal of Enology and Viticulture 2009, 60, 411-434.
- 404 7. May, P. From bud to berry, with special reference to inflorescence and bunch morphology in *Vitis vinifera*
405 L. Australian Journal of Grape and Wine Research 2000, 6, 82-98, doi:10.1111/j.1755-0238.2000.tb00166.x.
- 406 8. Rohde, A.; Bhalerao, R.P. Plant dormancy in the perennial context. Trends in Plant Science 2007, 12, 217-
407 223, doi:10.1016/j.tplants.2007.03.012.
- 408 9. Diaz-Riquelme, J.; Grimplet, J.; Martínez-Zapater, J.M.; Carmona, M.J. Transcriptome variation along bud
409 development in grapevine (*Vitis vinifera* L.). BMC Plant Biology 2012, 12.
- 410 10. Tarancón, C.; Gonzalez-Grandio, E.; Oliveros, J.C.; Nicolas, M.; Cubas, P. A Conserved Carbon Starvation
411 Response Underlies Bud Dormancy in Woody and Herbaceous Species. Frontiers in Plant Science 2017, 8,
412 788, doi:10.3389/fpls.2017.00788.

- 413 11. Barnett, T.; Altschuler, M.; McDaniel, C.N.; Mascarenhas, J.P. Heat shock induced proteins in plant cells.
414 Developmental Genetics 1980, 1, 331-340, doi:10.1002/dvg.1020010406.
- 415 12. Feder, M.E.; Hofmann, G.E. Heat-shock proteins, molecular chaperones, and the stress response:
416 evolutionary and ecological physiology. Annual Review Physiology 1999, 61, 243-282,
417 doi:10.1146/annurev.physiol.61.1.243.
- 418 13. Gupta, S.C.; Sharma, A.; Mishra, M.; Mishra, R.K.; Chowdhuri, D.K. Heat shock proteins in toxicology: how
419 close and how far? Life Sciences 2010, 86, 377-384, doi:10.1016/j.lfs.2009.12.015.
- 420 14. Tripp, J.; Mishra, S.K.; Scharf, K.D. Functional dissection of the cytosolic chaperone network in tomato
421 mesophyll protoplasts. Plant, Cell and Environment 2009, 32, 123-133, doi:10.1111/j.1365-3040.2008.01902.x.
- 422 15. Rushton, P.J.; Somssich, I.E.; Ringler, P.; Shen, Q.J. WRKY transcription factors. Trends in Plant Science
423 2010, 15, 247-258, doi:10.1016/j.tplants.2010.02.006.
- 424 16. Wang, M.; Vannozzi, A.; Wang, G.; Liang, Y.H.; Tornielli, G.B.; Zenoni, S.; Cavallini, E.; Pezzotti, M.; Cheng,
425 Z.M. Genome and transcriptome analysis of the grapevine (*Vitis vinifera* L.) WRKY gene family.
Horticulture Research 2014, 1, 14016, doi:10.1038/hortres.2014.16.
- 426 17. Jiang, J.; Ma, S.; Ye, N.; Jiang, M.; Cao, J.; Zhang, J. WRKY transcription factors in plant responses to stresses.
Journal of Integrative Plant Biology 2017, 59, 86-101, doi:10.1111/jipb.12513.
- 427 18. Dubos, C.; Stracke, R.; Grotewold, E.; Weisshaar, B.; Martin, C.; Lepiniec, L. MYB transcription factors in
428 Arabidopsis. Trends in Plant Science 2010, 15, 573-581, doi:10.1016/j.tplants.2010.06.005.
- 429 19. Matus, J.T.; Aquea, F.; Arce-Johnson, P. Analysis of the grape MYB R2R3 subfamily reveals expanded wine
430 quality-related clades and conserved gene structure organization across *Vitis* and *Arabidopsis* genomes.
BMC Plant Biology 2008, 8, 83, doi:10.1186/1471-2229-8-83.
- 431 20. Baldoni, E.; Genga, A.; Cominelli, E. Plant MYB Transcription Factors: Their Role in Drought Response
432 Mechanisms. Int J Mol Sci 2015, 16, 15811-15851, doi:10.3390/ijms160715811.
- 433 21. Masiero, S.; Colombo, L.; Grini, P.E.; Schnittger, A.; Kater, M.M. The emerging importance of type I MADS
434 box transcription factors for plant reproduction. The Plant Cell 2011, 23, 865-872,
435 doi:10.1105/tpc.110.081737.
- 436 22. Horvath, D.P. Dormancy-Associated MADS-BOX Genes: A Review. In Advances in Plant Dormancy,
437 Anderson, J.V., Ed. 2015; 10.1007/978-3-319-14451-1_7pp. 137-146.
- 438 23. Grimplet, J.; Martínez-Zapater, J.M.; Carmona, M.J. Structural and functional annotation of the MADS-box
439 transcription factor family in grapevine. BMC Genomics 2016, 17, 80, doi:10.1186/s12864-016-2398-7.
- 440 24. Wagner, D.; Sablowski, R.W.; Meyerowitz, E.M. Transcriptional activation of APETALA1 by LEAFY.
Science 1999, 285, 582-584, doi:10.1126/science.285.5427.582.
- 441 25. Kaufmann, K.; Wellmer, F.; Muino, J.M.; Ferrier, T.; Wuest, S.E.; Kumar, V.; Serrano-Mislata, A.; Madueno,
442 F.; Krajewski, P.; Meyerowitz, E.M., et al. Orchestration of floral initiation by APETALA1. Science 2010,
443 328, 85-89, doi:10.1126/science.1185244.
- 444 26. Vergara, R.; Noriega, X.; Parada, F.; Dantas, D.; Perez, F.J. Relationship between endodormancy,
445 FLOWERING LOCUS T and cell cycle genes in *Vitis vinifera*. Planta 2016, 243, 411-419, doi:10.1007/s00425-
446 015-2415-0.
- 447 27. Stafstrom, J.P.; Ripley, B.D.; Devitt, M.L.; Drake, B. Dormancy-associated gene expression in pea axillary
448 buds. Cloning and expression of PsDRM1 and PsDRM2. Planta 1998, 205, 547-552,
449 doi:10.1007/s004250050354.
- 450 28. Zhu, Y.; Wagner, D. Plant Inflorescence Architecture: The Formation, Activity, and Fate of Axillary
451 Meristems. Cold Spring Harbor Perspectives in Biology 2020, 12, a034652, doi:10.1101/cshperspect.a034652.
- 452 29. Quint, M.; Drost, H.G.; Gabel, A.; Ullrich, K.K.; Bönn, M.; Grosse, I. A transcriptomic hourglass in plant
453 embryogenesis. Nature 2012, 490, 98-101.
- 454 30. Drost, H.G.; Bellstädt, J.; Ó Maoiléidigh, D.S.; Silva, A.T.; Gabel, A.; Weinholdt, C.; Ryan, P.T.; Dekkers, B.J.;
455 Bentsink, L.; Hilhorst, H.W., et al. Post-embryonic Hourglass Patterns Mark Ontogenetic Transitions in
456 Plant Development. Molecular Biology and Evolution 2016, 33, 1158-1163.
- 457 31. Drost, H.G.; Janitza, P.; Grosse, I.; Quint, M. Cross-kingdom comparison of the developmental hourglass.
458 Current Opinion in Genetics & Development 2017, 45, 69-75.
- 459 32. Dudziak, K.; Sozoniuk, M.; Szczerba, H.; Kuzdralinski, A.; Kowalczyk, K.; Borner, A.; Nowak, M.
460 Identification of stable reference genes for qPCR studies in common wheat (*Triticum aestivum* L.) seedlings
461 under short-term drought stress. Plant Methods 2020, 16, 58, doi:10.1186/s13007-020-00601-9.

- 466 33. Lee, J.; Lee, I. Regulation and function of SOC1, a flowering pathway integrator. *Journal of Experimental*
467 *Botany* 2010, 61, 2247-2254, doi:10.1093/jxb/erq098.
- 468 34. Carmona, M.J.; Cubas, P.; Martínez-Zapater, J.M. VFL, the grapevine FLORICAULA/LEAFY ortholog, is
469 expressed in meristematic regions independently of their fate. *Plant Physiology* 2002, 130, 68-77.
- 470 35. Li-Mallet, A.; Rabot, A.; Geny, L. Factors controlling inflorescence primordia formation of grapevine: their
471 role in latent bud fruitfulness? A review. *Botany* 2016, 94, 147-163.
- 472 36. Daminato, M.; Masiero, S.; Resentini, F.; Lovisetto, A.; Casadore, G. Characterization of TM8, a MADS-box
473 gene expressed in tomato flowers. *BMC Plant Biology* 2014, 14, 319, doi:10.1186/s12870-014-0319-y.
- 474 37. Bogs, J.; Jaffe, F.W.; Takos, A.M.; Walker, A.R.; Robinson, S.P. The grapevine transcription factor
475 VvMYBPA1 regulates proanthocyanidin synthesis during fruit development. *Plant Physiology* 2007, 143,
476 1347-1361, doi:10.1104/pp.106.093203.
- 477 38. Koyama, K.; Numata, M.; Nakajima, I.; Goto-Yamamoto, N.; Matsumura, H.; Tanaka, N. Functional
478 characterization of a new grapevine MYB transcription factor and regulation of proanthocyanidin
479 biosynthesis in grapes. *Journal of Experimental Botany* 2014, 65, 4433-4449, doi:10.1093/jxb/eru213.
- 480 39. Wong, D.C.J.; Schlechter, R.; Vannozi, A.; Holl, J.; Hmam, I.; Bogs, J.; Tornielli, G.B.; Castellarin, S.D.;
481 Matus, J.T. A systems-oriented analysis of the grapevine R2R3-MYB transcription factor family uncovers
482 new insights into the regulation of stilbene accumulation. *DNA Research* 2016, 23, 451-466,
483 doi:10.1093/dnare/dsw028.
- 484 40. Vannozi, A.; Wong, D.C.J.; Holl, J.; Hmam, I.; Matus, J.T.; Bogs, J.; Ziegler, T.; Dry, I.; Barcaccia, G.;
485 Lucchin, M. Combinatorial Regulation of Stilbene Synthase Genes by WRKY and MYB Transcription
486 Factors in Grapevine (*Vitis vinifera* L.). *Plant and Cell Physiology* 2018, 59, 1043-1059,
487 doi:10.1093/pcp/pcy045.
- 488 41. Parage, C.; Tavares, R.; Rety, S.; Baltenweck-Guyot, R.; Poutaraud, A.; Renault, L.; Heintz, D.; Lugan, R.;
489 Marais, G.A.; Aubourg, S., et al. Structural, functional, and evolutionary analysis of the unusually large
490 stilbene synthase gene family in grapevine. *Plant Physiology* 2012, 160, 1407-1419,
491 doi:10.1104/pp.112.202705.
- 492 42. Yang, Y.; Zhang, L.; Chen, P.; Liang, T.; Li, X.; Liu, H. UV-B photoreceptor UVR8 interacts with
493 MYB73/MYB77 to regulate auxin responses and lateral root development. *EMBO Journal* 2019, 39, e101928,
494 doi:10.15252/embj.2019101928.
- 495 43. Chen, J.; Nolan, T.M.; Ye, H.; Zhang, M.; Tong, H.; Xin, P.; Chu, J.; Chu, C.; Li, Z.; Yin, Y. *Arabidopsis*
496 WRKY46, WRKY54, and WRKY70 Transcription Factors Are Involved in Brassinosteroid-Regulated Plant
497 Growth and Drought Responses. *The Plant Cell* 2017, 29, 1425-1439, doi:10.1105/tpc.17.00364.
- 498 44. Hernandez, L.D.; Vierling, E. Expression of Low Molecular Weight Heat-Shock Proteins under Field
499 Conditions. *Plant Physiol* 1993, 101, 1209-1216, doi:10.1104/pp.101.4.1209.
- 500 45. Lindquist, S. The heat-shock response. *Annual Review Biochemistry* 1986, 55, 1151-1191,
501 doi:10.1146/annurev.bi.55.070186.005443.
- 502 46. Burke, J.J.; Hatfield, J.L.; Klein, R.R.; Mullet, J.E. Accumulation of heat shock proteins in field-grown cotton.
503 *Plant Physiology* 1985, 78, 394-398, doi:10.1104/pp.78.2.394.
- 504 47. Hu, W.; Hu, G.; Han, B. Genome-wide survey and expression profiling of heat shock proteins and heat
505 shock factors revealed overlapped and stress specific response under abiotic stresses in rice. *Plant Science*
506 2009, 176, 583-590, doi:10.1016/j.plantsci.2009.01.016.
- 507 48. Swindell, W.R.; Huebner, M.; Weber, A.P. Transcriptional profiling of *Arabidopsis* heat shock proteins and
508 transcription factors reveals extensive overlap between heat and non-heat stress response pathways. *BMC*
509 *Genomics* 2007, 8, 125, doi:10.1186/1471-2164-8-125.
- 510 49. Jaillon, O.; Aury, J.M.; Noel, B.; Policriti, A.; Clepet, C.; Casagrande, A.; Choisne, N.; Aubourg, S.; Vitulo,
511 N.; Jubin, C., et al. The grapevine genome sequence suggests ancestral hexaploidization in major
512 angiosperm phyla. *Nature* 2007, 449, 463-467, doi:10.1038/nature06148.
- 513 50. Dobin, A.; Davis, C.A.; Schlesinger, F.; Drenkow, J.; Zaleski, C.; Jha, S.; Batut, P.; Chaisson, M.; Gingeras,
514 T.R. STAR: ultrafast universal RNA-seq aligner. *Bioinformatics* 2013, 29, 15-21.
- 515 51. Haak, M.; Vinke, S.; Keller, W.; Droste, J.; Rückert, C.; Kalinowski, J.; Pucker, B. High Quality de Novo
516 Transcriptome Assembly of *Croton tiglium*. *Frontiers in Molecular Biosciences* 2018, 5, 62.
- 517 52. Liao, Y.; Smyth, G.K.; Shi, W. featureCounts: an efficient general purpose program for assigning sequence
518 reads to genomic features. *Bioinformatics* 2014, 30, 923-930, doi:10.1093/bioinformatics/btt656.

- 519 53. Vitulo, N.; Forcato, C.; Carpinelli, E.C.; Telatin, A.; Campagna, D.; D'Angelo, M.; Zimbello, R.; Corso, M.;
520 Vannozzi, A.; Bonghi, C., et al. A deep survey of alternative splicing in grape reveals changes in the splicing
521 machinery related to tissue, stress condition and genotype. BMC Plant Biology 2014, 14, 99.
522 54. Barrett, P.; Hunter, J.; Miller, J.T.; Hsu, J.-C.; Greenfield, P. matplotlib – A Portable Python Plotting Package.
523 In Astronomical Data Analysis Software and Systems XIV ASP Conference Series, Proceedings of the
524 Conference held 24-27 October, 2004 in Pasadena, California, USA, Shopbell, P., Britton, M., Ebert, R., Eds.
525 Astronomical Society of the Pacific: San Francisco, 2005; Vol. 347, pp. 91-95.
526 55. Guo, C.; Guo, R.; Xu, X.; Gao, M.; Li, X.; Song, J.; Zheng, Y.; Wang, X. Evolution and expression analysis of
527 the grape (*Vitis vinifera* L.) WRKY gene family. Journal of Experimental Botany 2014, 65, 1513-1528,
528 doi:10.1093/jxb/eru007.
529
530



© 2020 by the authors. Submitted for possible open access publication under the terms and conditions of the Creative Commons Attribution (CC BY) license (<http://creativecommons.org/licenses/by/4.0/>).